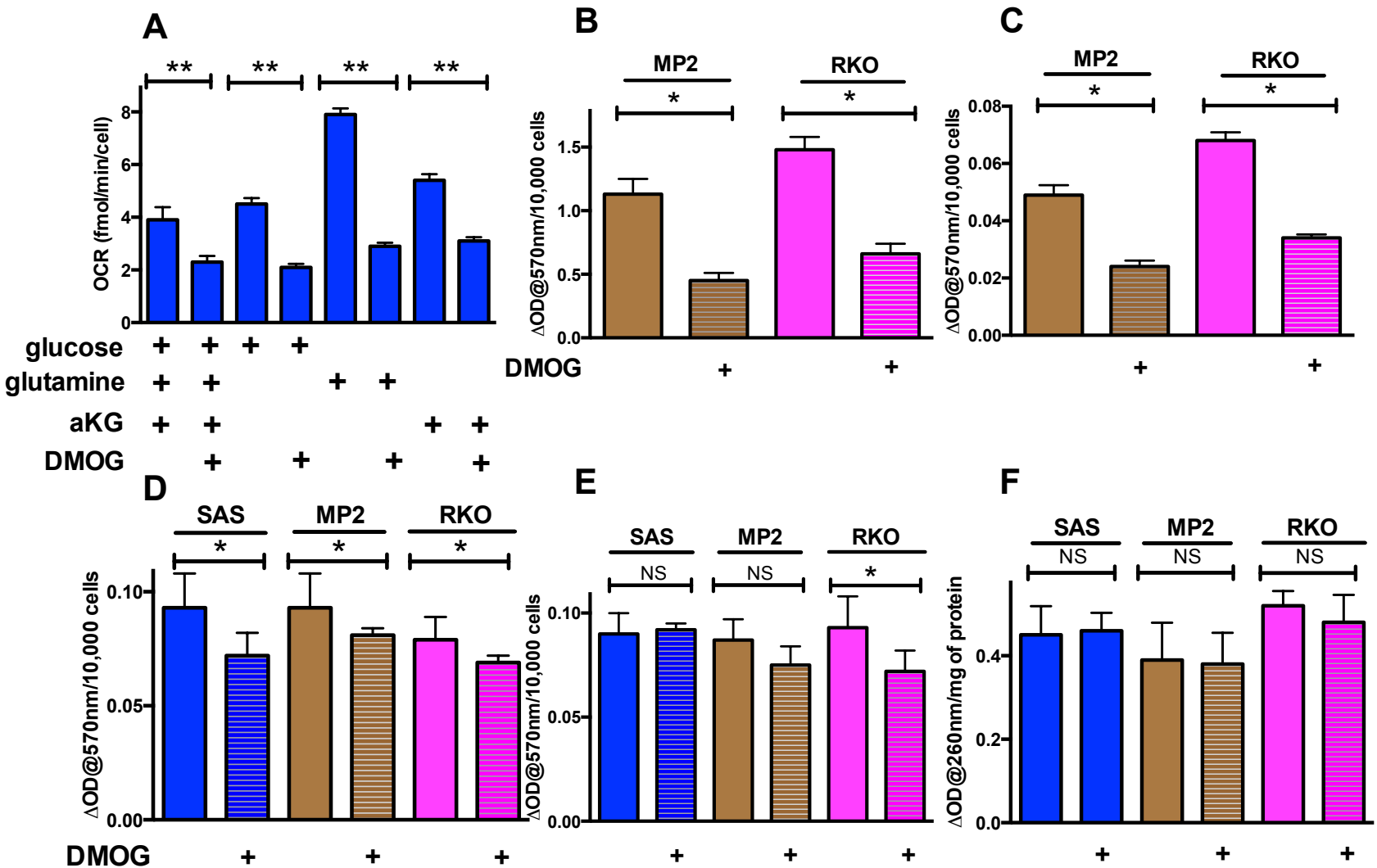
A
B
C
D
E
F
OCR (fmol/min/cell)
glucose
glutamine
aKG
DMOG
MP2
RKO
SAS
ΔOD@570nm/10,000 cells
ΔOD@260nm/mg of protein
NS

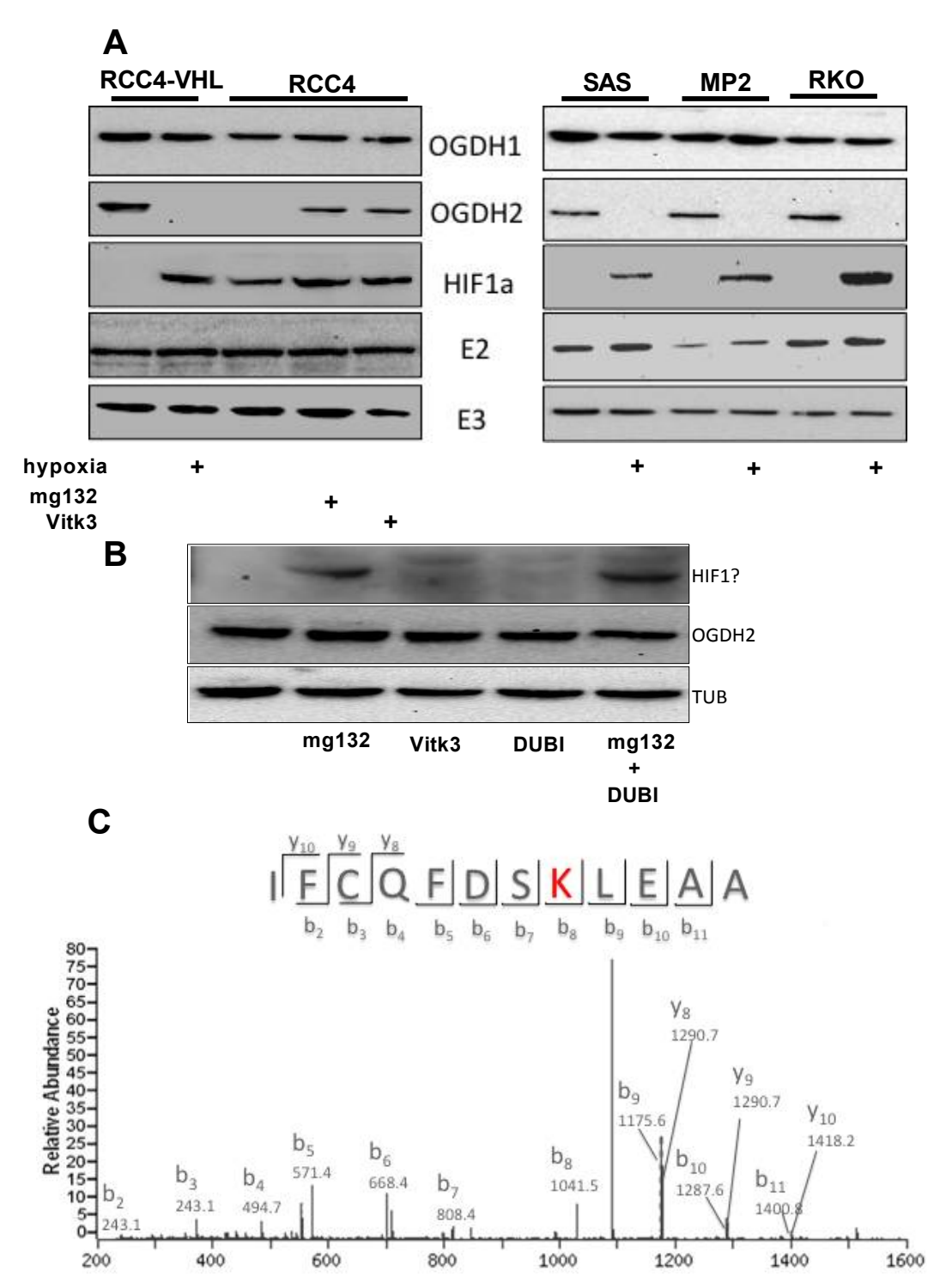
A
RCC4-VHL
RCC4
SAS
MP2
RKO
OGDH1
OGDH2
HIF1a
E2
E3
hypoxia
mg132
Vitk3
B
HIF1?
OGDH2
TUB
mg132
Vitk3
DUBI
mg132 + DUBI
C
IFCQFDSKLEAA
Relative Abundance
b2 243.1
b3 243.1
b4 494.7
b5 571.4
b6 668.4
b7 808.4
b8 1041.5
b9 1175.6
y8 1290.7
y9 1290.7
b10 1287.6
y10 1418.2
b11 1400.8

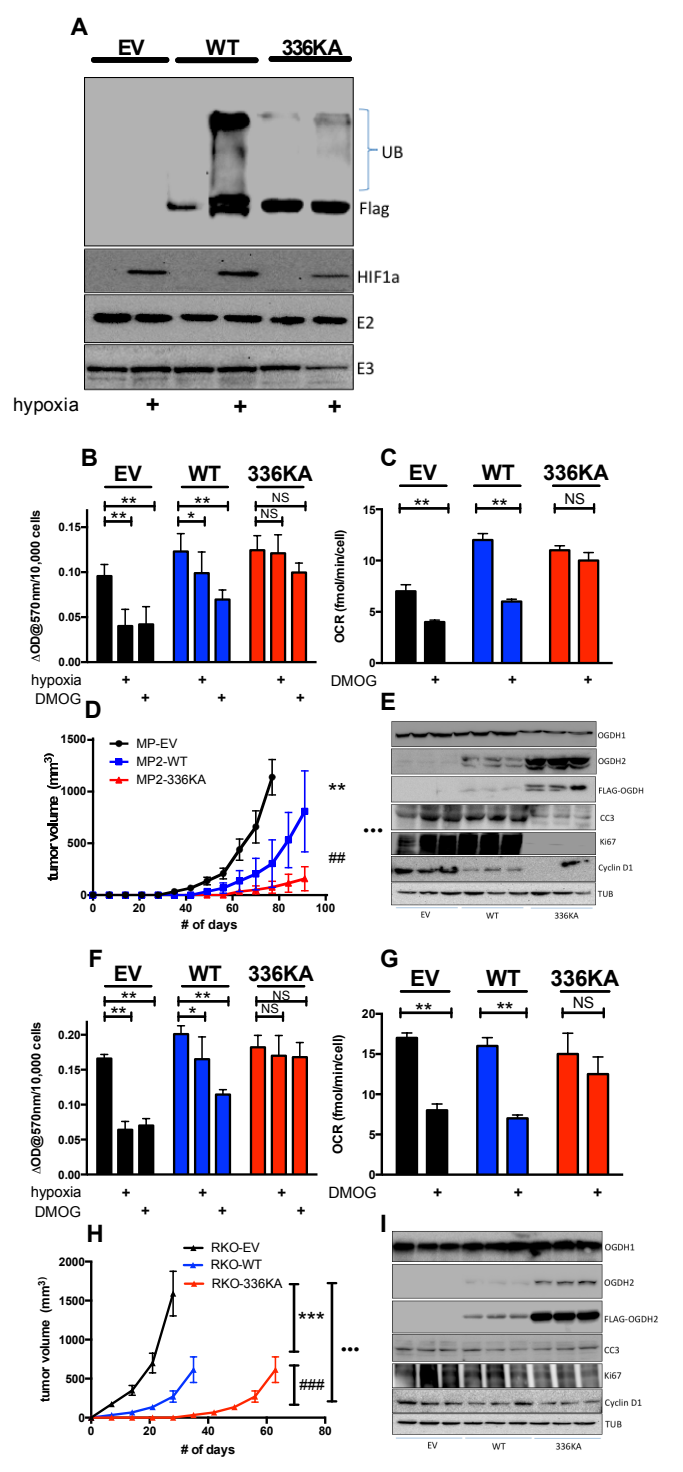
A
EV
WT
336KA
UB
Flag
HIF1a
E2
E3
hypoxia + + +
B
EV
WT
336KA
NS
ΔOD@570nm/10,000 cells
hypoxia
DMOG
C
OCR (fmol/min/cell)
D
MP-EV
MP2-WT
MP2-336KA
tumor volume (mm3)
# of days
E
OGDH1
OGDH2
FLAG-OGDH
CC3
Ki67
Cyclin D1
TUB
F
G
H
RKO-EV
RKO-WT
RKO-336KA
I

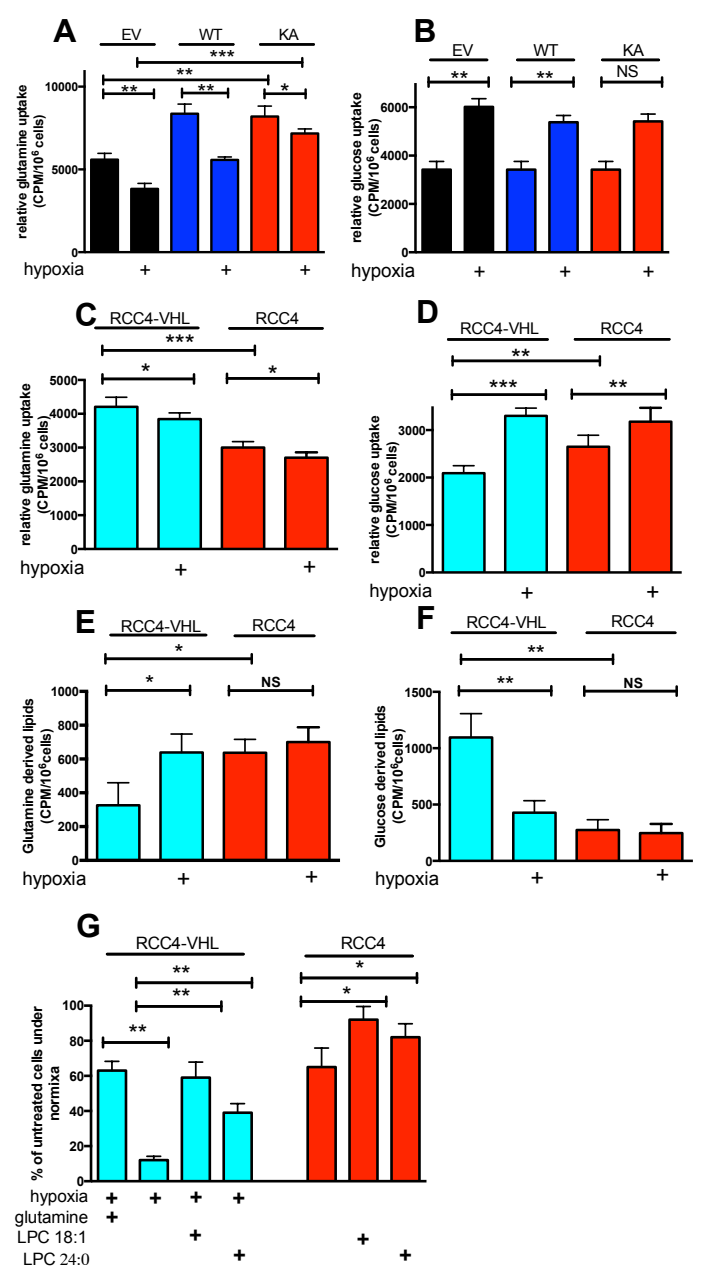
A
EV
WT
KA
***
**
**
**
*
relative glutamine uptake (CPM/10^6 cells)
10000
5000
0
hypoxia
+
+
+
B
EV
WT
KA
**
**
NS
relative glucose uptake (CPM/10^6 cells)
6000
4000
2000
0
hypoxia
+
+
+
C
RCC4-VHL
RCC4
***
*
*
relative glutamine uptake (CPM/10^6 cells)
5000
4000
3000
2000
1000
0
hypoxia
+
+
D
RCC4-VHL
RCC4
**
***
**
relative glucose uptake (CPM/10^6 cells)
3000
2000
1000
0
hypoxia
+
+
E
RCC4-VHL
RCC4
*
*
NS
Glutamine derived lipids (CPM/10^6cells)
1000
800
600
400
200
0
hypoxia
+
+
F
RCC4-VHL
RCC4
**
**
NS
Glucose derived lipids (CPM/10^6cells)
1500
1000
500
0
hypoxia
+
+
G
RCC4-VHL
RCC4
**
**
**
*
*
% of untreated cells under normixa
100
80
60
40
20
0
hypoxia
+
+
+
+
glutamine
+
LPC 18:1
+
+
LPC 24:0
+
+

Table S1 Putative mitochondrial proteins co-purified with OGDH2

Rank	Protein	score	Description
1	ODO1_HU	16821	2-oxoglutarate dehydrogenase, mitochondrial OS=Homo sapiens GN=OGDH PE=1 SV=3
2	ODO2_HU	1595	E2 component of 2-oxoglutarate dehydrogenase complex, mitochondrial OS=Homo sapiens GN=DLST PE=1 SV=4
3	TRAP1_H	324	Heat shock protein 75 kDa, mitochondrial OS=Homo sapiens GN=TRAP1 PE=1 SV=3
4	ATPA_HU	508	ATP synthase subunit alpha, mitochondrial OS=Homo sapiens GN=ATP5A1 PE=1 SV=1
5	GRP75_H	458	Stress-70 protein, mitochondrial OS=Homo sapiens GN=HSPA9 PE=1 SV=2
6	ATPB_HU	309	ATP synthase subunit beta, mitochondrial OS=Homo sapiens GN=ATP5B PE=1 SV=3
7	AATM_HU	143	Aspartate aminotransferase, mitochondrial OS=Homo sapiens GN=GOT2 PE=1 SV=3
8	THIL_HUM	94	Acetyl-CoA acetyltransferase, mitochondrial OS=Homo sapiens GN=ACAT1 PE=1 SV=1
9	TIM13_HU	81	Mitochondrial import inner membrane translocase subunit Tim13 OS=Homo sapiens GN=TIMM13 PE=1 SV=1
10	AIFM1_H	73	Apoptosis-inducing factor 1, mitochondrial OS=Homo sapiens GN=AIFM1 PE=1 SV=1
11	KCRU_HU	70	Creatine kinase U-type, mitochondrial OS=Homo sapiens GN=CKMT1A PE=1 SV=1
12	TIM8A_H	64	Mitochondrial import inner membrane translocase subunit Tim8 A OS=Homo sapiens GN=TIMM8A PE=1 SV=1
13	ODPB_HU	57	Pyruvate dehydrogenase E1 component subunit beta, mitochondrial OS=Homo sapiens GN=PDHB PE=1 SV=3
14	CH60_HU	57	60 kDa heat shock protein, mitochondrial OS=Homo sapiens GN=HSPD1 PE=1 SV=2
15	ATPG_HU	55	ATP synthase subunit gamma, mitochondrial OS=Homo sapiens GN=ATP5C1 PE=1 SV=1
16	NDUS3_H	51	NADH dehydrogenase [ubiquinone] iron-sulfur protein 3, mitochondrial OS=Homo sapiens GN=NDUFS3 PE=1 SV=1
17	ECHA_HU	48	Trifunctional enzyme subunit alpha, mitochondrial OS=Homo sapiens GN=HADHA PE=1 SV=2
18	P5CR1_HU	45	Pyrroline-5-carboxylate reductase 1, mitochondrial OS=Homo sapiens GN=PYCR1 PE=1 SV=2
19	GUF1_HU	44	Translation factor GUF1, mitochondrial OS=Homo sapiens GN=GUF1 PE=1 SV=1
20	THIM_HU	43	3-ketoacyl-CoA thiolase, mitochondrial OS=Homo sapiens GN=ACAA2 PE=1 SV=2
21	M2OM_H	42	Mitochondrial 2-oxoglutarate/malate carrier protein OS=Homo sapiens GN=SLC25A11 PE=1 SV=3
22	EFTU_HU	42	Elongation factor Tu, mitochondrial OS=Homo sapiens GN=TUFM PE=1 SV=2
23	ETFA_HU	40	Electron transfer flavoprotein subunit alpha, mitochondrial OS=Homo sapiens GN=ETFA PE=1 SV=1
24	ECI1_HUM	35	Enoyl-CoA delta isomerase 1, mitochondrial OS=Homo sapiens GN=ECI1 PE=1 SV=1
25	GLYM_HU	35	Serine hydroxymethyltransferase, mitochondrial OS=Homo sapiens GN=SHMT2 PE=1 SV=3

Supplemental figure legends.

Figure S1 Mitochondrial enzyme activities after HIF stabilization, related to figure 1.

Panel A: Mitochondrial OCR in RCC4 VHL cells in media containing various mitochondrial substrates after treatment with 500 uM DMOG. Note either cells in αKG alone or with αKG in full media both show reduced OCR after HIF stabilization.

Panel B: αKGDH activity in MiaPaca2 and RKO cells from control and DMOG treated cultures (500μM 16h).

Panel C: Pyruvate dehydrogenase activity In MiaPaca2 and RKO cells from control and DMOG treated cultures.

Panel D: Glutamate dehydrogenase activity in SAS, MiaPaca2 and RKO cells from control and DMOG treated cultures.

Panel E: NADP+ dependent Isocitrate dehydrogenase activity in SAS MiaPaca2 and RKO cells from control and DMOG treated cultures.

Panel F: NADPH dependent αKG reductive carboxylation activity in SAS, MiaPaca2 and RKO cells from control and DMOG-treated cultures. All error bars represent standard deviation.

Figure S2 OGDH2 modification and destruction in response to hypoxia, related to figure 2.

Panel A: Left side, western blot of extracts from RCC4-VHL cells after treatment with hypoxia, and RCC4 cells in normoxia that have been treated with either proteasome inhibitor MG132, or SIAH2 inhibitor VitK3. Right side, Western blot of extracts from SAS, Miapaca2 and RKO cells from control, and hypoxia-treated cultures as indicated. Membranes were probed with OGDH1/3, OGDH2, DLST(E2), DLD(E3), and HIF1 as indicated.

Panel B: western blot of extracts from normoxic SAS cells, treated with either 10μM MG132, 50μM VitK3 or 10μM DUBI and MG132 as indicated. Membranes were probed with HIF1, OGDH2 as indicated.

Panel C: Peptide sequence from the spectrograph of immunopurified OGDH2 after treatment with hypoxia, MG132 and DUBI. Modified lysine in peptide is residue 336.

Figure S3 Expression of a hypoxia-resistant OGDH2 (336KA) blocks the hypoxic glutamine response and inhibits tumor growth, related to figure 3.

Panel A Western blot of extracts from SAS cells expressing empty vector, Flag-WT OGDH2 or Flag-336KA OGDH2 from normoxic or hypoxic cultures treated with MG132 and DUBI probed with a-Flag to detect the polyubiquitinated species of OGDH2.

Panel B: αKGDH activity in MP2 cells expressing either empty vector, WT OGDH2, or 336KA in normoxic DMOG-treated or hypoxic cultures.

Panel C: Mitochondrial OCR in MP2 cells described in B, in either control, or DMOG-treated cultures.

Panel D: Tumor growth of MP2 cells described in B after injection into immune-deficient mice (n=8-10 tumors per group) Error bars represent standard error of the mean.

Panel E: Western blot of extracts from explanted tumors desdcribed in panel D grown from MP2 cells expressing either empty vector, OGDH2 WT or OGDH2 336KA as indicated. Blots probed with indicated antibodies.

Panel F: αKGDH activity in RKO cells expressing empty vector, WT OGDH2, or 336KA in normoxic DMOG-treated or hypoxic cultures.

Panel G: Mitochondrial OCR in RKO cells described in E, in either control, or DMOG-treated cultures.

Panel H: Tumor growth of RKO cells described in E after injection into immune-deficient mice (n=8-10 tumors per group). Error bars represent standard error of the mean.

Panel I Western blot of extracts from explanted tumors desdcribed in panel H grown from RKO cells expressing either empty vector, OGDH2 WT or OGDH2 336KA as indicated. Blots probed with indicated antibodies. Error bars from panels B, C, F, and G represent standard deviation.

Figure S4 Shift in metabolic substrate utilization after HIF stabilization, related to figure 4.

Panel A: Radiolabelled glutamine uptake in SAS cells expressing empty vector, WT OGDH2 or 336KA OGDH2 in control and hypoxia-treated cultures.

Panel B: Radiolabelled glucose uptake in SAS cells expressing empty vector, WT OGDH2 or 336KA OGDH2 in control and hypoxia-treated cultures

Panel C: Radiolabelled glutamine uptake in RCC4-VHL and RCC4 cells from normoxic or hypoxic cultures

Panel D: Radiolabelled glucose uptake in RCC4-VHL and RCC4 cells from normoxic or hypoxic cultures

Panel E: Radiolabelled glutamine incorporation into lipids in RCC4-VHL and RCC4 cells in normoxic or hypoxic cultures.

Panel F: Radiolabelled glucose incorporation into lipids in RCC4-VHL and RCC4 cells from normoxic or hypoxic cultures.

Panel G Rescue of glutamine-dependent hypoxic growth with the addition of desaturated lysophospholipids in the media for RCC4-VHL cells and RCC4 cells grown in normoxia. Error bars in all panels represent standard deviation.

Table S1 Mitochondrial proteins co-purifying with OGDH2 after immune-precipitation, identified by mass spectroscopy. Confidence scores are a function of the number of identified peptides from each protein, data is related to figures 3 and S3.

Supplemental Methods

Dehydrogenase assays. Dehydrogenase activity was assessed using a whole cell colorimetric assay previously described [1], which measures NADH/NADPH generated from specific substrates. Reducing equivalents are used to convert nitroblue tetrazolium in the presence of phenazine methosulfate into an insoluble blue formazan precipitate which is then solubilized in 0.01N HCL in 10% SDS to determine OD. Cells were seeded in 96 well plates at 10^4/well and treated over night at 37^{o}C. The next day cells were permeabilised with 0.5% triton X-100 in PBS, followed by incubation with the reaction buffer for 30min-60min in a 37^{o}C CO_2 incubator. After incubation cells were washed 3 times and the blue fomazan was dissvoled in 10% SDS in 0.01N HCL over night. OD at 570 nm was obtained using the SpectraMAX 190 spectrophotometer (Molecular Devices, CA, USA). Reaction buffer for PDH activity consists of 5 mM 3-bromopyruvate (to inhibit glycolytic production of pyruvate and NADH) 1mM $MgCl_2$, 0.05mM EDTA, 0.2% triton X-100, 0.3 mM ThDP, 10µM rotenone, 10mM pyruvate, 3mM NAD, 1mM Co-A, 0.75 mM NBT and 0.05mM PMS in 50mM Tris-Hcl pH7.8. Reaction for αKGDH and GDH were similar, except for removal of pyruvate, and addition of 10mM αKG or glutimate respectively. Reaction buffer for NAD/NADP IDH activities consists of 8mM MgCl2, 1mM MnCl2, 0.05mM EDTA, 0.2% triton X-100, 10 µM rotenone, 2mM NAD/0.5mM NADP, 1.5 mM isocitrate, 10mM citrate, 2mM ADP, 0.75mM NBT and 0.05mM PMS in 50mM tris-Hcl pH7.5.

NAP+ IDH reductive activity assay. 10^7 cells were lysed and IDH was extracted by 1ml of extraction buffer (10mM MgCl2, 5mM mecaptoethanol, 1mM EDTA, 5mM MnCl2, 2mM ADP 5M glycerol in 50mM pipes buffer pH 7.8), cell extracts were centrifuged and 100ul of the supernatant was added to 1ml of reaction buffer (8mM $MgCl_2$, 1mM $MnCl_2$, 3mM aKG, 0.5nM NADPH), and OD at 260 was obtained by a SpectraMAX spectrophotometer.

Proliferation Assays. To measure proliferation rate, 10^4 viable cells were plated in a 12-well plates in triplicate. Cells were counted 72 hours post plating and the number of viable cells was determined by trypan blue exclusion.

Site-mapping of OGDH2 ubiquitination. 10^7 MP2 cells stabily expressing Flag-OGDH2 were cultured under 0.5% oxygen overnight and for the last three hours, mg132 and DUBI (nsc632839) was added. Cells were lysed in RIPA buffer and Flag-OGDHV2 was IP-ed with M2 flag

antibody (Sigma), captured using protein A/G PLUS (Santa Cruz Biochemical) and fractionated on a 10%-acrylamide gel. Protein bands were detected with Xypro Ruby and molecules between 45-60kDa were identified and the bands picked by the Ettan Spot Handling Work station 2.1. Gel pieces were washed in 50% methanol/5% acetic acid followed by acetonitrile and dried. The gel fragment was suspended in 50 mM ammonium bicarbonate buffer, the proteins reduced with DTT, treated with iodoacetamide, dried and suspended in 50 mM ammonium bicarbonate for in gel digestion with trypsin (sequencing grade Promega) for 6 hours at 37ºC. The peptides were extracted from the polyacrylamide with 50 µL 50% acetonitrile and 5% formic acid three times. A final extraction with 50 µL of acetonitrile was performed. The extracted pool was completely dried and peptides were resuspended in 22 µL of 50 mM acetic acid.

The peptides were analyzed using capillary-liquid chromatography-nanospray tandem mass spectrometry (Capillary-LC/MS/MS). Global protein identification was performed on a Thermo Finnigan LTQ orbitrap mass spectrometer equipped with a microspray source (Michrom Bioresources Inc, Auburn, CA) operated in positive ion mode. Sample (6.4 µL from each fraction) were separated on a capillary column (0.2X150mm Magic C18AQ 3µ 200A, Michrom Bioresources Inc, Auburn, CA) using an UltiMate™ 3000 HPLC system from LC-Packings A Dionex Co (Sunnyvale, CA). Each sample was injected into the µ-Precolumn Cartridge (Dionex, Sunnyvale, CA) and desalted with 50 mM acetic acid. The peptides were eluted off of the trap onto the column. Mobile phase A was 50mM acetic acid in water and acetonitrile was mobile phase B. Flow rate was set at 2µl/min. Mobile phase B was increased stepwise to 90% over 90 minutes. The column was equilibrated between samples. MS/MS data was acquired with a spray voltage of 2.2 KV and a capillary temperature of 175 ºC. The scan sequence of the mass spectrometer was based on the data dependent TopTen™ method in preview mode: the analysis was programmed for a full scan recorded between 400-2,000 Da and a MS/MS scan to generate product ion spectra to determine amino acid sequence in consecutive scans of the ten most abundant peaks in the spectrum. Dynamic exclusion is enabled with a repeat count of 1 within 18 s, a mass list size limit of 500, exclusion duration of 10 s and a low mass width and high mass width were set at 30ppm. The RAW data files were converted to mzXML and MGF files by use of MassMatrix[1] data conversion tools (version 1.3), For low mass accuracy data, tandem MS spectra that were not derived from singly charged precursor ions were considered as both doubly and triply charged precursors. The resulting mgf files were searched for human proteins in the Swiss Port database (20, 233 sequences) using Mascot Daemon by Matrix Science version 2.2.1 (Boston, MA). The mass accuracy of the precursor ions were set to 1.8 Da given that the data

was acquired on an ion trap mass analyzer and the fragment mass accuracy was set to 0.8 Da. Considered modifications were methionine oxidation (variable), deamidation (variable), ubiquitination (variable) and carbamidomethyl cysteine (fixed). Two missed cleavages for the enzyme were permitted. Additionally, the .dat files from Mascot were loaded into Scaffold and an additional screen for ubiquitinated peptides was performed.

Immunoblot Assays. Protein lysates were extracted with RIPA buffer supplemented with Complete-Mini protease inhibitor (Roche) and quantified by BCA Protein Assay (Pierce). Samples were resolved on SDS polyacrylamide gel and transferred to PVDF membrane. Samples were analyzed by immunoblotting with antibodies for HIF1α (BD Bioscience), OGDH1/3 (abcam), OGDH2 (abcam), E2 (abcam), E3 (abcam) , SIAH2 (Sigma) and FLAG (Sigma).

Glutamine/glucose uptake. 10^5 cells were treated and then incubated with 5μCi of ^{14}C-glucose or ^{14}C-glutamine for 5 min at 37^{o}C in a 5% CO_2 incubator in media containing 1mM glutamine, 5mM glucose supplemented with charcoal stripped serum. After incubation, cells were placed on ice, washed 3 times with cold PBS, and lysed with 200ul of 0.2%SDS/0.2N NaOH. Total counts were determined with a scintillation counter (PerkinElmer Life Sciences).

Site directed mutagenesis. Lysine 336 was changed to alanine using the QuickChange2 site-directed mutagenesis kit (Agilent technologies) following manufacture's protocols. Briefly, Flag-OGDH2 in pCMV was amplified by PCR using forward primer: GTCAATTCGATTCAGCGCTGGAGGCAGCTG and reverse primer: CAGCTGCCTCCAGCGCTGAATCGAATTGAC, following PCR original methylated DNA plasmid was digested by DpNI, and the remaining product was transformed in to XL10-Gold competent cells. Plasmid with the correct mutation was confirmed by sequencing before being used for transfection.

Statistical Analysis. Unless otherwise noted, data are presented as the mean ± SD. Statistical significance was determined with two-sample Student's t test comparing experimental conditions to appropriate controls. Statistical significance was determined at a value of

* $0.01 < p < 0.05$

** $0.001 < p < 0.01$

*** $p < 0.001$

1. Mayer, K.M. and F.H. Arnold, *A colorimetric assay to quantify dehydrogenase activity in crude cell lysates.* J Biomol Screen, 2002. **7**(2): p. 135-40.